Scholar Publishing Group
Kinetic Mechanical Engineering
https://doi.org/10.38007/KME.2022.030104
ISSN 2790-2676 Vol. 3, Issue 1: 28-37

Design of an All-electric Bus Cooling System Incorporating Computational Fluid Dynamics

Kim Davide*

University of Turin, Italy

**corresponding author*

Keywords: Computational Fluid Dynamics, Electric Bus, Cooling System, Optimal Design

Abstract: With the emphasis on renewable energy and environmental protection, new energy vehicles are gradually entering the social space and electric vehicles are once again moving to new heights. The aim of this paper is to investigate the design of a cooling system for a purely electric bus incorporating computational fluid dynamics. This paper follows the principle of "determine the heat source distribution of the prototype - calculate the temperature rise of the prototype - design an optimised cooling structure - analyse the cooling effect - propose the design of the prototype cooling structure". This paper studies the temperature rise and cooling of the prototype, focusing on the effect of different cooling structures on the temperature rise of the prototype. Based on the heat transfer, a finite element model of the engine is established and the losses and heat source distribution of the prototype are calculated by combining empirical equations and MAP diagrams of the engine losses. The heat transfer process of the engine is investigated, including the heat transfer process within and between the components of the prototype in contact with each other, and the convective heat transfer process between the prototype and the fluid contact surface. Based on the CFD (Computational Fluid Dynamics) method, the flow and temperature fields of the physical air-cooled prototype are calculated using the existing CFD mathematical model, and the influence of the flow field of the prototype heat exchanger ventilation duct on the engine temperature rise is analysed. A forced air cooling solution for the prototype was proposed to determine the structure of the vents, the location of the ventilation holes and the size of the cooling fan. The effect of forced air cooling on the temperature rise of the prototype is compared with the effect of natural air cooling. A parallel water jacket should be designed and its structure optimised in order to compare the effect of the water jacket on the temperature rise of the prototype before and after optimisation. Finally, all studies are combined to provide reference recommendations for the design of the prototype cooling structure.

1. Introduction

It is well known that after the development of the automobile, the first real motor vehicle in the world was the electric car. However, the internal combustion engine vehicle came later and with the rapid development of fuel technology, its superior overall performance and high cost, beat the electric vehicle in the automotive market. Initially, electric vehicles were mainly used in applications where the overall performance of the vehicle was not required and these applications showed the advantages of electric vehicles, such as quiet operation and zero emissions. In recent years, with the increasing environmental pollution problems and the transformation of traditional industries, electric vehicles have gradually become an advantage for the automotive industry, but due to technical problems in the development of power batteries, the development of electric vehicles was very slow in the early stages of development. In recent years, with the development of battery technology, a large number of pure electric vehicles have emerged [1-2].

In the study of the design of pure electric bus cooling system incorporating computational fluid dynamics, many scholars have studied it with good results, e.g. Bhowmik P K The design method should be validated by comparing experimental results with computational results. The design method should be validated by comparing experimental results with computational results [3]. Habashi W G compared the conventional flat fin and the new hybrid fin cooler by numerical calculations and experimental validation and found that the fin cooler dissipated heat better than the flat fin cooler under the same operating conditions [4].

This paper follows the principle of "determine the heat source distribution of the prototype - calculate the temperature rise of the prototype - design an optimised cooling structure - analyse the cooling effect - propose the design of the prototype cooling structure". This paper studies the temperature rise and cooling of the prototype, focusing on the effect of different cooling structures on the temperature rise of the prototype. Based on the heat transfer, a finite element model of the engine is established and the losses and heat source distribution of the prototype are calculated by combining empirical equations and MAP diagrams of the engine losses. The heat transfer process of the engine is investigated, including the heat transfer process within and between the components of the prototype in contact with each other, and the convective heat transfer process between the prototype and the fluid contact surface. Based on the CFD (Computational Fluid Dynamics) method, the flow and temperature fields of the physical air-cooled prototype are calculated using the existing CFD mathematical model, and the influence of the flow field of the prototype heat exchanger ventilation duct on the engine temperature rise is analysed. A forced air cooling solution for the prototype was proposed to determine the structure of the vents, the location of the ventilation holes and the size of the cooling fan. The effect of forced air cooling on the temperature rise of the prototype is compared with the effect of natural air cooling. A parallel water jacket should be designed and its structure optimised in order to compare the effect of the water jacket on the temperature rise of the prototype before and after optimisation. Finally, all studies are combined to provide reference recommendations for the design of the prototype cooling structure.

2. Research on the Design of a Cooling System for Pure Electric Buses Incorporating Computational Fluid Dynamics

2.1. Viscosity of the Fluid

Viscosity is the property of a fluid to resist the shear forces acting on it. There are two ways of expressing viscosity: the kinetic (absolute) viscosity μ and the kinematic viscosity υ, which are related as follows [5-6].

$$\nu = \frac{\mu}{\rho} \tag{1}$$

Where: μ - dynamic viscosity coefficient in Pa-s; ν - kinematic viscosity coefficient in m2/s; ρ - fluid density in kg/m3.

The force generated by viscosity is internal friction, also known as viscous drag. Newton's law of internal friction defines the expression for the tangential stress between two layers of fluid as

$$\tau = \mu \frac{du}{dy} \tag{2}$$

Where: τ - shear stress in N; $\frac{du}{dy}$ - velocity gradient in 1/s perpendicular to the contact surface of the two fluid layers.

2.2. The Solution Process of the CFD

The CFD solving process generally consists of three main parts: pre-processing, solving and post-processing, of which the STAR-CCM+ solving process can be represented by the following flow chart [7-8]. As shown in figure 1.

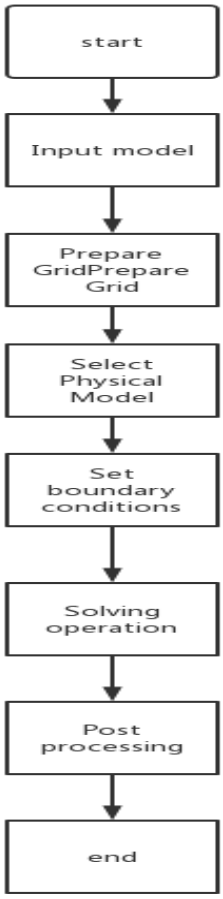

Figure 1. Solving the flow chart

2.3. Heat Transfer within the Controller

The heat during the operation of the motor controller is mainly generated by the high-power power electronics, and the heat of the subject of this paper mainly originates from the IGBT. for the purpose of heat dissipation in engineering, the high-power power electronics are generally installed directly on the heat sink, and the heat is transferred from the substrate and the heat-conducting silicone grease to the heat sink and then taken away by the cooling medium. the influence of radiation on heat dissipation in this process can be ignored, and thus the main heat dissipation methods are Heat conduction and thermal convection [9-10].

The heat transfer process consists of two main parts: one in which heat is transferred from a higher temperature part to a lower temperature part within the same component, and the other in which heat is transferred from a higher temperature part to a lower temperature part between the contact surfaces of different components. The convective heat exchange process also consists of two parts: one part is the heat exchange process between the radiator and the cooling medium; the other part is the natural convective heat exchange between the housing and the outside air. If the cooling method is forced water cooling, the forced convection heat transfer effect of the water is much stronger than the natural convection effect of the air outside the housing, so most of the heat generated by the chip inside the IGBT will be carried away by the convection heat exchange of the cooling medium after it has been transferred to the heat sink by heat conduction [11-12].

3. Research and Design Experiments on the Design of Cooling Systems for Pure Electric Buses Incorporating Computational Fluid Dynamics

3.1. Principle of the Experimental System

The motor-to-trailer test stand is used to test the performance of the drive motor and its controller. The test stand is equipped with measuring instruments and equipment such as vibration analysers, noise analysers and power analysers to analyse the temperature, vibration, voltage and efficiency of the motor and controller. The system consists of seven subsystems: the main circuit system, the system under test, the accompanying test system, the control system, the test system, the cooling system and the auxiliary system. The accompanying test system, also known as the dynamometer system, is an important part of the motor to tractor test rig [13-14]. It is used to simulate the resistance and inertial load of the vehicle during the driving process after the motor has been loaded, and to determine the performance of the system under test. The motor under test and the accompanying motor are connected via specific half-shaft adapters to form a motor-to-drag system with a torque flange mounted on the shaft and equipped with a speed-torque detection unit for real-time detection and feedback of speed and torque signals. The rectifier, the motor controller and the motor and the accompanying motor controller and the accompanying motor are electrically connected to each other. The signal acquisition and control during the test is carried out via the host computer and CAN communication. The platform is equipped with a test switching power supply to power the system under test and the accompanying system, and to recover the electrical energy generated during the operation of the motor [15-16]. The cooling system consists of an industrial thermostatic cooler, which provides a circulating coolant of a certain temperature and flow rate for the motor controller, the motor under test, the accompanying motor controller and the accompanying motor during the experiment. The dynamometer used in this experiment is an AC power dynamometer, which consists of a load mechanism, a test mechanism, a control mechanism, an operation and safety mechanism, a simulation mechanism and related accessories.

3.2. Experimental Procedure

The experiment was carried out according to the following steps.

(1) Testing of the insulation impedance of the motor and controller to ensure that the motor can complete the experiment successfully.

(2) Complete the installation and construction of the motor and controller and the test stand: all mechanical parts should be installed and fixed tightly, firmly and without looseness, to ensure that the prototype and instruments are placed smoothly and neatly, and the two sets of motors need to ensure sufficient concentricity; the connection of high-voltage cables and low-voltage harnesses should be tight and without looseness, and the connection should be well insulated, and the wiring should be checked for correct connection after completion; the connection of water pipes should be tight and without looseness, and the wiring should be checked for correct connection after completion. The connection of water pipes should be tight and free from looseness, and the wiring should be checked for correct line connection after completion, and the water should be run for a test run to check for leaks [17-18].

(3) Turn on the cooling circulation equipment (industrial thermostat cooler), set the flow rate and temperature according to the test requirements and make sure there are no leakage points in the whole water circuit. Set the initial coolant temperature to 60 ℃ and the coolant flow rate to 15L/min to ensure consistency with the actual working conditions.

(4) Turn on the voltage supply and confirm that the low voltage current is normal when the controller is not driven.

(5) Open the upper computer of the pair of towers, select the corresponding device type, baud rate and CAN channel, check whether the motor information fed back in the motor information area is normal, then start the high-voltage DC power supply, set the voltage to the voltage required for the test, and observe whether the voltage value collected by the controller is normal through the upper computer. After the high voltage power-up is complete, select the test voltage condition to be performed, measure the temperature near the IGBT heat source using the thermistor measurement points on the controller itself, measure and record the data.

(6) After the test is started, observe whether the towing system operates normally, whether the motor feedback information is normal, whether any faults are reported, whether the data is saved normally, and monitor normal operation for at least 30 minutes.

(7) When the operation is completed and stopped, click the stop operation confirmation button, and when the torque and speed have completely stopped, turn off the low voltage power supply, turn off the high voltage DC power supply, turn off the upper computer and turn off the cooling circulation equipment.

(8) Complete the experiment and organize the laboratory equipment.

4. Experimental Analysis of the Design of a Pure Electric Bus Cooling System Incorporating Computational Fluid Dynamics

4.1. Data Analysis

The electric drive system under test was operated at rated power and peak speed conditions, and some data on the temperature of the controller IGBT module was recorded as a function of time, with the temperature of the motor and controller rising and reaching equilibrium during bench operation. The motor and controller temperatures are plotted against running time as shown in Figures 2 and 3.

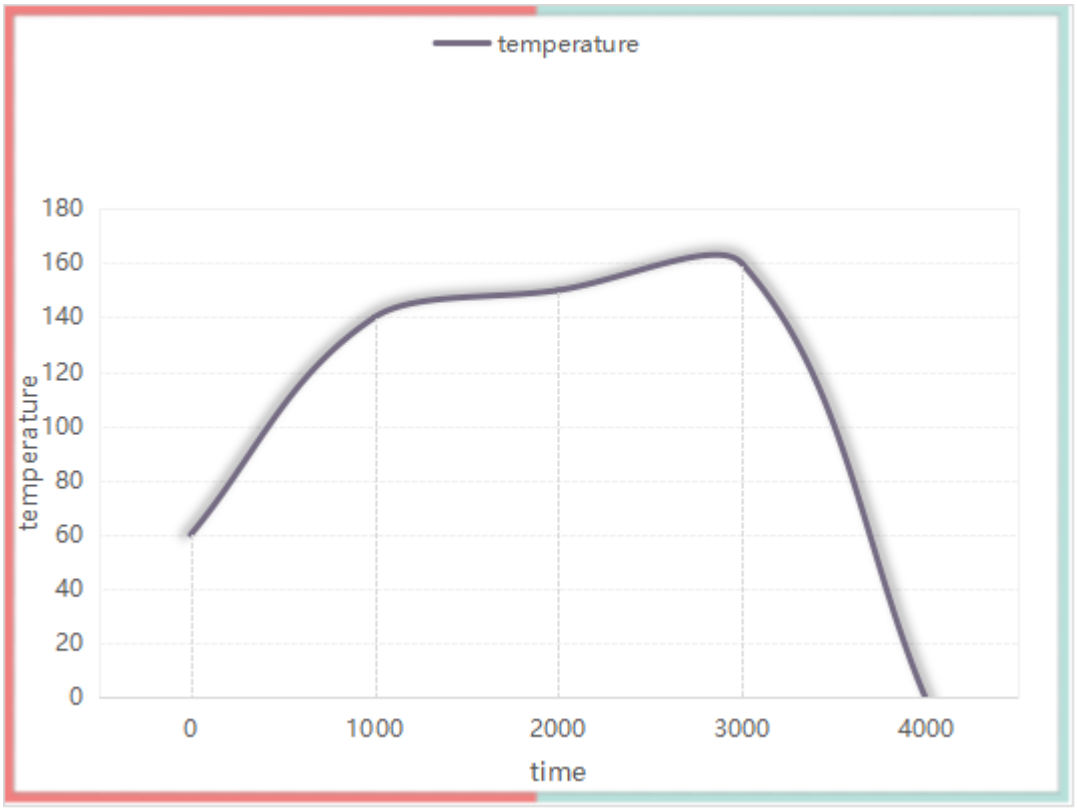

Figure 2. Motor temperature change diagram

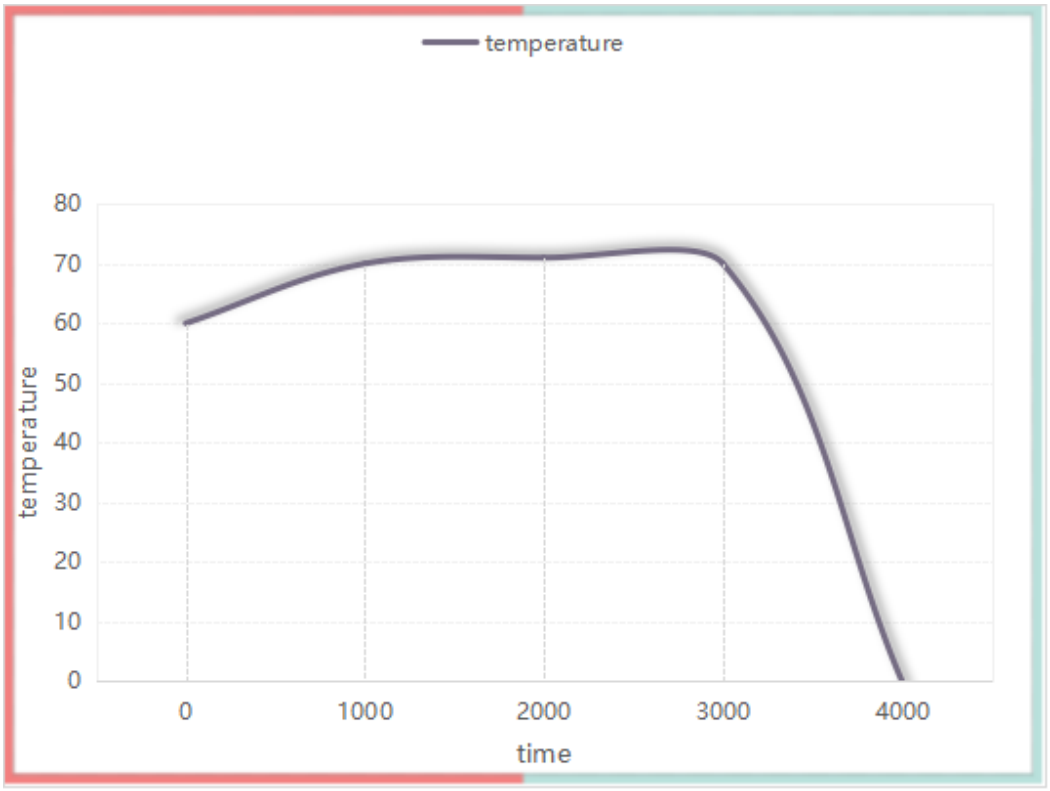

Figure 3. Temperature change map of the controller

As can be seen from the graph, the temperature rise of the motor rises continuously to 161 ℃ during operation and the controller temperature soon stabilises at around 71 ℃.

4.2. Comparison of Results and Error Analysis

The temperature measured by the sensor in the test is located near the chip, the temperature measured is not the temperature of the chip itself, according to experience can be increased by 10 ℃ for the chip temperature, then the test measured temperature is 81 ℃. In the simulation process, the temperature value near the temperature sensor measurement point is taken, which is similar to the temperature measured under the actual test. By comparing the experimental results of the temperature rise with the simulation results, it can be seen that the simulation values are higher than the actual measured values. The experimental data is shown in Table 1.

Table 1. Comparison of theory, simulation and experiment

	Chip temperature	Chip temperature error rate	NTC temperature	NTC temperature error rate
Verify the measured data	81	0	71	0
theoretical arithmetic	85.6	5.7	75.1	5.9
numerical simulation	85	4.9	73	2.8

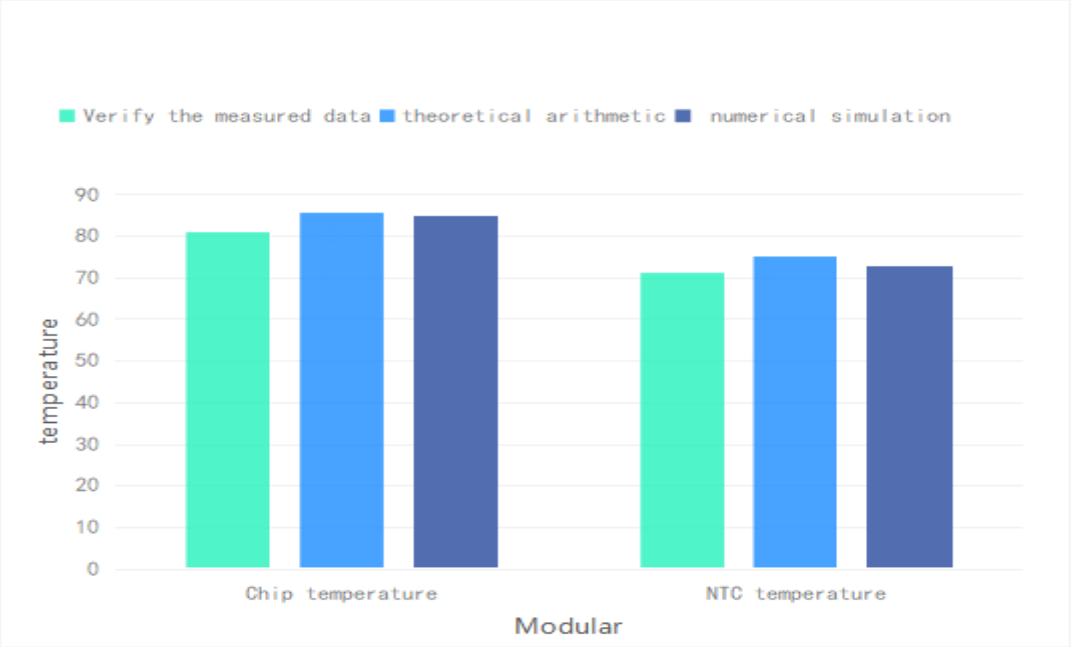

Figure 4. Comparison of errors between simulation and calculation and measured temperature

Figure 4 shows that the theoretical calculated chip temperature is 4.6℃ higher than the experimental value with an error of 5.7%, and the simulated temperature of 85℃ is 4℃ higher than the experimental value with an error of 4.9%, so the theoretical and simulated results of thermal resistance can be considered reliable.

The error is absolutely present and will not be eliminated, so we need to analyse the error of the experiment. The simulation values are higher than the experimental values and the errors arise from both experimental and simulation errors.

(1) The error in the experimental process mainly stems from the systematic error of the experimental equipment, some control errors in the process and the environment.

1) Systematic errors in experimental equipment mainly arise from measurement errors, such as errors in the accuracy of thermistor measurements and rounding errors in computers.

2) The speed of operation during the process and the control of the industrial thermostatic cooling system in ensuring constant temperature and flow rate may cause the actual value to fluctuate back and forth around the expected setting value, affecting the experimental results.

3) In addition, the ambient temperature of the outside world can also have an impact on the experiment.

(2) The errors in the accuracy of the simulation results are mainly due to the errors in the calculation of the heat loss of the module, the errors in the calculation of the equivalent thermal conductivity and the equivalent physical properties of the DBC plate when it is simplified, and the errors caused by the quality of the mesh division in the software during the calculation process.

1) Loss calculation errors: Since it is difficult to calculate the losses of IGBTs in actual operating conditions accurately, there are undoubtedly errors in the resulting heat loss power.

2) Simplification and equivalence errors: Due to the many layers of DBC plate structure and complex materials, in order to save calculation time and make the simulation go smoothly, the corresponding simplification and equivalence of DBC may be different from the actual situation, resulting in errors in the calculation results.

3) Software accuracy errors: When the finite element software is used for simulation calculations, the mesh quality varies due to different mesh settings, as well as the choice of convergence settings and calculation methods can bring about differences in calculation results.

5. Conclusion

This paper focuses on the temperature field problem of a high-power motor controller for a pure electric bus, and the cooling system design by investigating the heat source, thermal field and heat dissipation structure. On top of this, the temperature and fluid fields are studied visually and visually using professional CFD software, and the accuracy of the theory and simulation is verified through experiments. The main work and conclusions of this paper are summarised as follows: (1) Review the relevant literature on the current state of research in controller cooling systems at home and abroad, study and briefly introduce the ways of heat transfer and the control equations of computational fluid dynamics, so as to lay a good foundation for the successful completion of the thesis. (2) To analyze the heat transfer mode of the controller cooling system, establish a thermal resistance model, and use experiments to determine the magnitude of the thermal resistance value, so as to facilitate rapid estimation of the operating temperature of the IGBT chip and save a lot of test and labor costs. (3) Selecting the cooling scheme and system arrangement based on losses, and studying the effects of materials, cooling media and different water channel structures and rib structures on the heat dissipation effect. The optimisation of the radiator size selection is completed by orthogonal tests to reduce the motor controller operating temperature, improve the controller operating performance and ensure efficient, stable and reliable operation of the controller. (4) The

design of the heat sink system for the IGBT high power module is based on CAD/CAE software. The controller and the main components of its cooling system are modelled using the 3D software Pro/E, and the simulation of the fluid and temperature fields is completed using the professional CFD software STAR-CCM+ to ensure the rationality of the design. (5) Conduct a motor-to-motor test to test the temperature rise of the motor controller during actual operation to verify the accuracy and reliability of the simulation calculations.

Funding

This article is not supported by any foundation.

Data Availability

Data sharing is not applicable to this article as no new data were created or analysed in this study.

Conflict of Interest

The author states that this article has no conflict of interest.

References

[1] Vaishnav S , Kapadiya V , Harish R , et al. Design and analysis of energy-efficient solar panel cooling system using computational fluid dynamics. IOP Conference Series: Materials Science and Engineering, 2021, 1128(1):012033 (14pp).https://doi.org/10.1088/1757-899X/1128/1/012033

[2] Mi B G , Huang H . Intake grille design for an embedded ventilation-and-cooling system in an aircraft. Proceedings of the Institution of Mechanical Engineers, Part G: Journal of Aerospace Engineering, 2022, 236(11):2352-2365. https://doi.org/10.1177/09544100211062810

[3] Bhowmik P K , Schlegel J P , Kalra V , et al. CFD validation of condensation heat transfer in scaled-down small modular reactor applications, Part 1: Pure steam. Experimental and Computational Multiphase Flow, 2022, 4(4):409-423. https://doi.org/10.1007/s42757-021-0115-5

[4] Habashi W G , Targui A . On a reduced-order model-based optimization of rotor electro-thermal anti-icing systems. International Journal of Numerical Methods for Heat & Fluid Flow, 2022, 32(8):2885-2913. https://doi.org/10.1108/HFF-06-2021-0417

[5] Zhang Q , Yang H , Ding L , et al. Failure Mechanism and Flow Field of Choke Manifold in a Natural Gas Well: Computational Fluid Dynamic Simulation. Arabian Journal for Science and Engineering, 2022, 47(9):12103-12115. https://doi.org/10.1007/s13369-022-06897-0

[6] Dinarvand S , Nejad A M . Off-centered stagnation point flow of an experimental-based hybrid nanofluid impinging to a spinning disk with low to high non-alignments. International Journal of Numerical Methods for Heat & Fluid Flow, 2022, 32(8):2799-2818. https://doi.org/10.1108/HFF-09-2021-0637

[7] Chen D , Cheng P . Development of design system for product pattern design based on Kansei engineering and BP neural network. International Journal of Clothing Science and Technology, 2022, 34(3):335-346. https://doi.org/10.1108/IJCST-04-2021-0044

[8] Mousavian R , Mashhadi Hossainali M , Lorenz C , et al. Copula, a new approach for optimum design of Voxel-based GNSS tropospheric tomography based on the atmospheric dynamics. GPS Solutions, 2022, 26(4):1-17. https://doi.org/10.1007/s10291-022-01340-1

[9] Dey S , Banerjee S , Dey J . Design of an improved robust fractional order PID controller for magnetic levitation system based on atom search optimization. Sādhanā, 2022, 47(4):1-19. https://doi.org/10.1007/s12046-022-01962-8

[10] Wang G , Zhu B , Fan Y , et al. Design and evaluation of an exergame system to assist knee disorders patients' rehabilitation based on gesture interaction. Health Information Science and Systems, 2022, 10(1):1-10. https://doi.org/10.1007/s13755-022-00189-5

[11] Celik F A . A new design of SiO2-Na2O-Al2O3 glass-ceramic and determination of elastic modulus and density of states via molecular dynamics simulations based on density functional tight-binding calculations. Journal of the Korean Ceramic Society, 2022, 59(5):647-654. https://doi.org/10.1007/s43207-022-00201-4

[12] Research on Design and Control of Dual-Energy Source System for Pure Electric Vehicle. IOP Conference Series: Materials Science and Engineering, 2020, 799(1):012036 (7pp). https://doi.org/10.1088/1757-899X/799/1/012036

[13] Karimi T , Yahyazade Y . Developing a risk assessment model for banking software development projects based on rough-grey set theory. Grey Systems: Theory and Application, 2022, 12(3):574-594. https://doi.org/10.1108/GS-05-2021-0074

[14] Buragohain M , Das N K D . A neoteric closed loop feedback controller based on correlative-elemental curvature algorithm. Circuit World, 2022, 48(3):341-353. https://doi.org/10.1108/CW-06-2020-0107

[15] Ghosh S K , Singh S . Pressure drop and heat transfer characteristics in 60 ° Chevron plate heat exchanger using Al2O3, GNP and MWCNT nanofluids. International Journal of Numerical Methods for Heat & Fluid Flow, 2022, 32(8):2750-2777. https://doi.org/10.1108/HFF-08-2021-0580

[16] Yang X , Hu Y , Liu Z . Enhancing turbulence: a potential strategy for drag reduction based on ground transportation systems (GTS) model. International Journal of Numerical Methods for Heat & Fluid Flow, 2022, 32(8):2819-2840. https://doi.org/10.1108/HFF-06-2021-0387

[17] Ebrahimpour Z , Sheikholeslami M , Farshad S A . Heat transfer within linear Fresnel unit using parabolic reflector. International Journal of Numerical Methods for Heat & Fluid Flow, 2022, 32(8):2841-2863. https://doi.org/10.1108/HFF-05-2021-0338

[18] Kai-Tao H E , Zhi-Zhong L I , Wang D M . Overview on the Design of the Service and Management System for Field Geological Survey Based on the Remote Sensing and Beidou Satellites. Journal of Geomechanics, 2022, 18(3):203-212.